ELECTRICAL PROPERTIES OF JUNCTIONS BETWEEN ALUMINUM AND POLY[3-(2'-BUTYLOXY-5'-(1'''-OXOOCTYL)PHENYL)THIOPHENE]

A Thesis Submitted to the

School of Graduate Studies

Addis Ababa University

In Partial Fulfillment

of the Requirements for the Degree

of Master of Science in Physics

By

Mandefro Yehulie

June 2003

Addis Ababa

ADDIS ABABA UNIVERSITY

SCHOOL OF GRADUATE STUDIES

ELECTRICAL PROPERTIES OF JUNCTIONS BETWEEN ALUMINUM AND POLY [3-(2'-BUTYLOXY-5'-(1'''-OXOOCTYL)PHENYL)THIOPHENE].

By

Mandefro Yehulie

Department of Physics

Faculty of Science

APPROVED BY THE EXAMINATION COMMITTEE

Name	**Signature**
Dr. Bantikassegn Workalemahu, Advisor	_____
Prof. S. K. Sharma, Examiner	_____
Prof. Singh P., Examiner	_____

Acknowledgement

I would like to express my deep gratitude and appreciation to my instructor and advisor Dr. Bantikassegn Workalemahu, for introducing me to the field of Conjugated Polymer Physics, excellent guidance, encouragement, and material support. I gratefully acknowledge him for providing me convenient working environment, well-equipped laboratory, journals, and other materials.

I would like to thank the Department of Physics, Addis Ababa University.

My sincere thank goes to BahirDar University.

I would like to express my sincere thanks to the International Program in the Physical Science (IPPS) for equipping research laboratory with all the necessary materials.

I extend my thanks to Dr. Wondimagegn Mammo at Department of Chemistry, Addis Ababa University.

I am also indebted to thank my friends:

- Bekalu Mola and Tesfaye Ayalew for introducing me to the laboratory work.
- Girmachew Adugna for his unlimited support and encouragement.

Abstract

The electrical properties of junctions between a low work function metal (Al) and poly[3-(2'-butyloxy-5'-(1'''-oxooctyl)phenyl)thiophene] in the form of Al/polymer/ITO sandwich structures have been investigated by means of complex impedance spectroscopy, current-voltage (I-V), and capacitance-voltage (C-V) characteristics. The current–voltage curve is non-ohmic and reveals Schottky barrier type of rectification. The C-V data together with I-V characteristics confirms the polymer is a p-type semiconducting polymer. The complex impedance spectroscopy shows the absence of an insulating interfacial resistive layer. Schottky device parameters have been calculated from I-V curve by applying the thermionic emission equation. As result, saturation current density $(J_0) = 2.2\times10^{-13}\ A/cm^2$, ideality factor (n) = 3.5, rectification ratio = 1761, built-in voltage = 0.96V, potential barrier = 1.11eV, dopant density $(N_a) = 4.83\times10^{17}\ cm^{-3}$, and depletion width at zero bias voltage = 25.7nm have been deduced from our experimental data.

Table of Contents **page**

List of Tables page

List of Figures page

1. Introduction

Organic polymers are long molecules consisting of carbon atoms as a backbone and having very high molecular weight, often measured in hundreds of thousands gm/mole. They are called macromolecules. These large molecules are made from small molecules called monomers through polymerization process.

Until about thirty years ago all carbon based polymers were regarded as insulators. Hence, they were used as inactive packaging and insulating materials. However, in 1976, Alan MacDiarmid, Hideki Shirakawa and Alen J. Heeger together with a talented group of graduate students and post-doctorial researchers discovered conducting polymers and the ability to dope these polymers over a full range from insulator to metal [1, 2]. This discovery created a new field of research on the boundary between chemistry and condensed matter physics. The idea that plastics could be made to conduct electricity would have been considered to be absurd. But, plastics have been extensively used by electronics industry because of this property.

Pure organic polymers or undoped polymers are insulators (or semiconductor) and have a filled valance band and an empty conduction band. Research work on undoped or doped conjugated polymers, such as polyacetylene [3], polypyrole [4], polyaniline [5], and polythiophene and its derivatives [6,7] have shown semiconducting behavior that can be used in device applications. Examples of such systems are the pn junctions [8], Schottky barrier diode [9], field effect transistor [10], and polymer light-emitting diodes [11].

Conducing polymers are π-conjugated polymers and they have variety of structures. The extensive delocalization of π-electrons and variety of structures are well known to be

responsible for the array of remarkable characteristics that these polymers tend to exhibit. These properties lead them to be applicable in fields of thin film technology, synthetic metals, electroluminescence, non-linear optics, and many more.

Conjugated polymers are highly susceptible to chemical or electrochemical oxidation or reduction. These alter the electrical and optical properties of the polymer, and by controlling this oxidation and reduction**,** it is possible to precisely control these properties. For instance, doping of polyacetylene with AsF_5 increased its conductivity to 10^5S/cm, which is near to the conductivity of copper. The relative conductivities of some of the polymers synthesized are shown below.

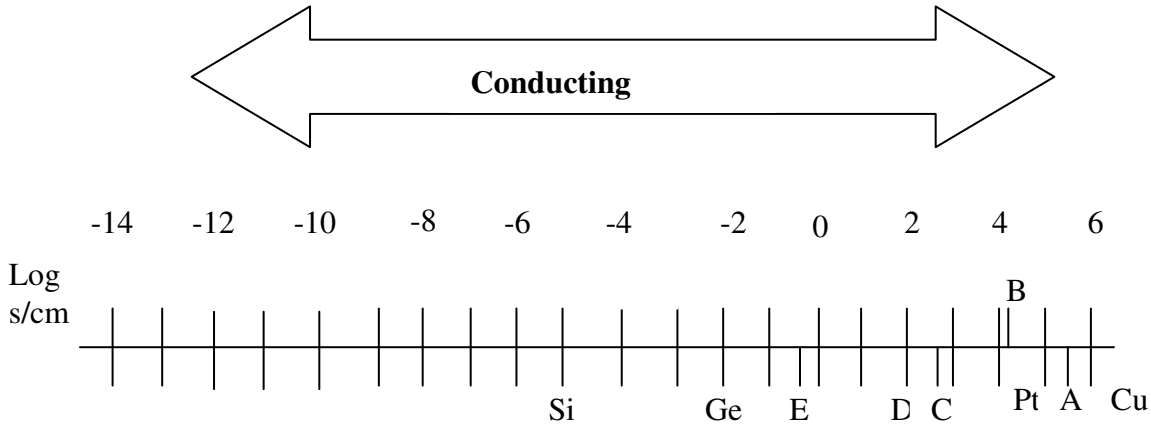

Fig. 1. 1. Range of conductivity of polymers compared with conductivities of other materials at room temperature. Points A, B, C, D and E indicate the conductivity of polyacetylene doped with AsF_5, polyacetylene doped with I_2, poly (p-phenylene) doped with AsF_5, polypyrrole doped with I_2 and polyaniline respectively.

Problems in the development of many applications are low stability and lack of easy processability. Much research will be needed before many of the applications will become a reality. To overcome these problems research effort has been directed towards the synthesis of well-defined conjugated polymers (and oligomers) by adding appropriate side chains, which significantly improves the properties, processability, and /or environmental stability. For instance, in polythiophene, a variety of side chain substituents attached to the 3- and/ or 4-positions give rise to processability and modified electronics properties. Some of substituted polythiophene are poly[3-(4-octylphenyl))-2,2'-biothiophene], PTOPT, poly(3-octylphenylthiophene), POPT, poly(3-4-ethylenedioxythiophene), PEDOT. These polymers have generated significant progress in electroluminescence [12] and electrochromism [13].

The objective of this research work is to study the absorption spectrum of poly[3-(2'-butyloxy-5'-(1'''-oxooctyl)phenyl)thiophene], and the electronic properties of junctions between aluminum and the polymer. The polymer is one of the derivatives of polythiophene synthesized in the department of chemistry of Addis Ababa University. It has a side chain to give rise to solubility and easy processability and modified electronic properties.

The method used to achieve the objective of the research has two major steps. The first is preparation of the sample, which involves use of spinner system, Edwards Auto 306 Vacuum Depositor, and others. The second aspect is characterization where by sample is characterized by measuring absorption spectrum, current-voltage (I-V), capacitance-voltage (C-V), and complex impedance spectroscopy.

The current-voltage, capacitance-voltage, and complex impedance data are analyzed using standard theories of physics of semiconductor devices.

2. Conjugated Polymers

2.1 Conjugated Polymers

Conjugated polymers are class of materials that have strictly alternating single and double bonds. Some examples of conjugated polymers are shown below. Polyacetylene is

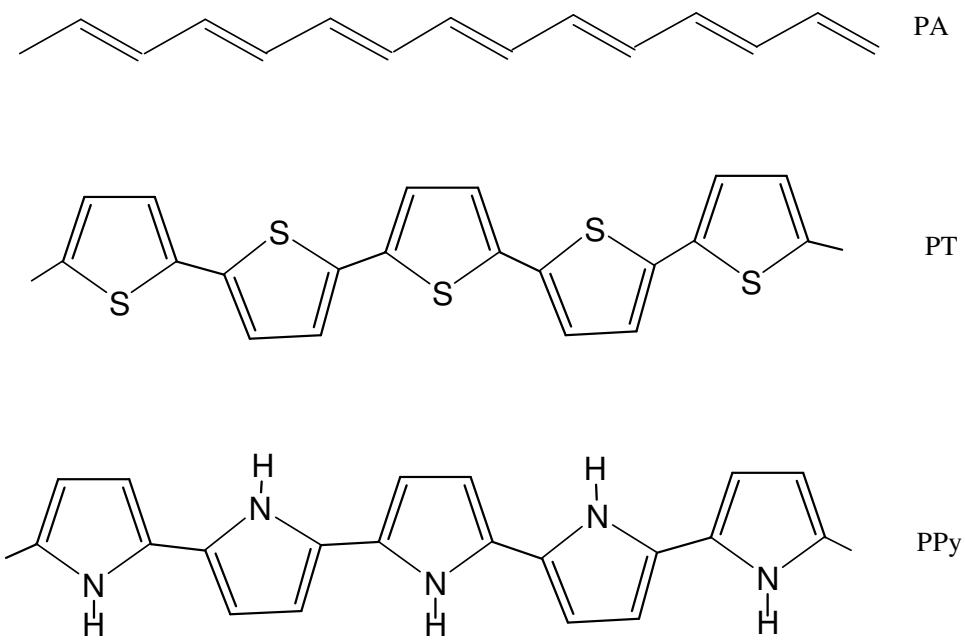

Fig. 2. 1. Chemical structures of alternating single and double bonds in conjugated polymers a) Polyacetylene=PA b) polythiophene=PT c) polypyrrole=PPy

one of the most well known conjugated polymers. The conductivity of polyacetylene, when it is highly doped, is the highest of all conducting polymers so far observed, which is as high as that of copper [14]. It has the most regular and most symmetric structure of all conjugated polymers. It is the first polymer to be observed conducting [1]. From its optical absorption spectra measurement, the π-π^* gap (or the band gap) was found to be about 1.7eV, which is in the region of known inorganic semiconductor [15].

In general the conductivity of conjugated polymers is not high along the chains of alternating bonds. Because of strong and localized double bonds. Therefore, pure conjugated polymers are insulators or semiconductors. Furthermore, these polymers are quasi-one-dimensional

chains. Thus, to have a clear picture about these polymers, we need to study the physics of one-dimensional solids.

2.2 Hybridization

In order to explain the existence of the structure of atoms and molecules that corresponds to geometric pattern predicted from Valance Shell Electron Pair Repulsion (VSEPR) theory, chemists have found it necessary to develop hybridization theory. Hybridization theory says that atoms involved in the formation of covalent bond will undergo structural changes in their atomic orbitals of valence level. Thus, hybridization is the process of combining two or more atomic orbitals to create new orbitals, called hybrids, which will fulfill the geometric demand of the characteristics but differ somewhat in their geometric configuration.

In the formation of hydrogen molecule from two separate hydrogen atoms, atomic orbitals overlap. Let's consider the overlap of 1s atomic orbitals of two electrons of hydrogen atoms. These orbitals can combine in two different ways. The first way is when the two nuclei of the two hydrogen atoms brought together to a distance equal to the interatomic distance in the molecules, and the wave functions of the two 1s electrons summed to give the wave function of the molecule. Just as shown in Fig.2.2 below, cylindrically symmetric geometry about the line joining the two nuclei called σ-molecular orbital is formed. The bond formed is called σ-bond and the energy level is called the Highest Occupied Molecular, or π, Orbital (HOMO). The second way of combination is when the wave function of 1s atomic orbital of electron of the first hydrogen atom is subtracted from 1s atomic orbital of the electron of the second hydrogen atom. This type of molecular orbital is called antibonding molecular orbital. Its

energy level is called the Lowest Unoccupied Molecular, π*, Orbital (LUMO).

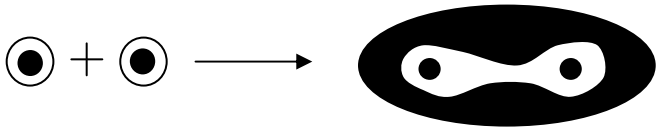

Fig. 2. 2. Cylindrically symmetric σ-bonding of a hydrogen molecule.

When the energy of antibonding and bonding MOs are calculated, it is found that the energy of bonding MO is less than the energy of the electrons in the constituent atomic 1s orbitals while the antibonding MO energy is greater than the atomic orbitals' energy by the same amount like that of bonding MO is less from the atomic orbitals. That is, the bonding MO is stable while the antibonding MO is unstable. We can apply Pauli's exclusion principle for molecular orbitals like atomic orbitals. This may be shown on an energy level diagram of formation of H_2 as shown in the Fig. 2.3 below.

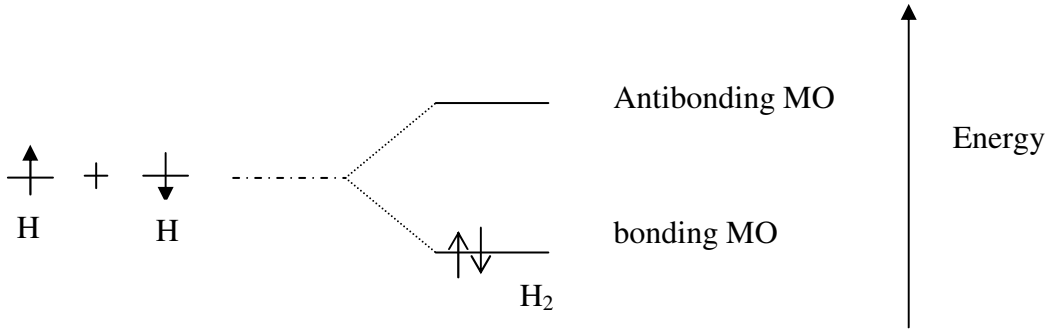

Fig. 2. 3. Energy schematics showing the overlap of 1s atomic orbitals of two H atoms

to form a bonding and antibonding molecular orbital of H_2.

The second type of bonding MO can be formed by the overlap or combination of two atomic 2p orbitals. Particularly, the combination of two $2p_z$ orbitals gives π- bonding MO and π^*-antibonding MO. The π-bonding MO and π^*-antibonding MO have influences on the properties of conjugated polymers.

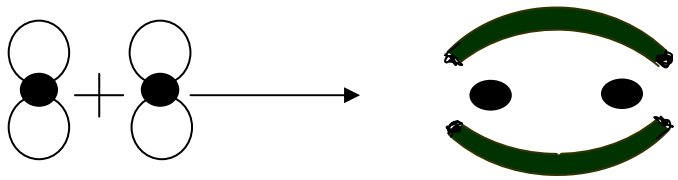

Fig. 2. 4. Overlap of two p_z orbitals to give π-bonding MO.

The use of pure s and p atomic orbitals fails to account for the shape of most molecules (e.g. linear, triangular, or tetrahedral shapes). Therefore, hybridization of atomic orbitals, which is a new concept, has to be introduced for understanding the nature of covalent bond. Instead of atomic orbitals, hybrid orbitals overlap more effectively and form strong bonds. For instance, in methane (CH_4), a carbon atom has four electrons in its valence shell, and these electrons form covalent bonds with electrons of four hydrogen atoms. The ground state electronic configuration of C-atom is $1s^2 2s^2 2p^2$. When 2s orbital is superimposed with three 2p ($2p_x$, $2p_y$, $2p_z$) orbitals, four equivalent hybrid orbitals, called sp^3 hybrid orbitals, will be formed. The sp^3 hybrid orbitals will align along the corners of the tetrahedral as in the Fig 2.5 below. The overlap of 1s atomic orbitals of hydrogen atoms with these sp^3 hybrids will form σ-bond molecular orbitals and covalent C-H bonds.

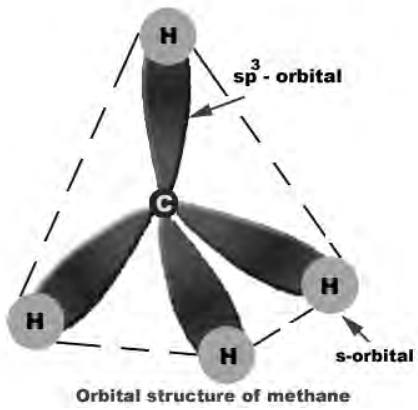

Fig. 2. 5. The sp^3 hybridized carbon atom in methane.

In a similar way, mixing process can be carried out with s orbital and two of 2p orbitals ($2p_x$, $2p_y$) to give three equivalent sp^2 hybrid orbitals separated by 120^0. Such hybridization occurs, for example, in ethylene as shown in the Fig.2.6. Two sp^2 hybrid orbitals form σ-covalent bond with 1s atomic orbitals of hydrogen atoms and the other sp^2 hybrid form σ-bond with the sp^2 hybrid of neighboring carbon atom. The remaining $2p_z$ orbital of carbon atom, by overlapping with $2p_z$ orbital of the other neighboring carbon atom, forms covalent bond called the π-bond. Consequently, it yields smaller separation between bonding (HOMO-Highest Occupied MO) and antibonding (LUMO-Lowest Unoccupied MO) MOs. There is also another class of hybridization called sp hybridization that occurs, for instance, in acetylene.

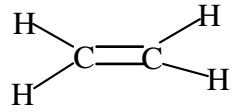

Ethylene

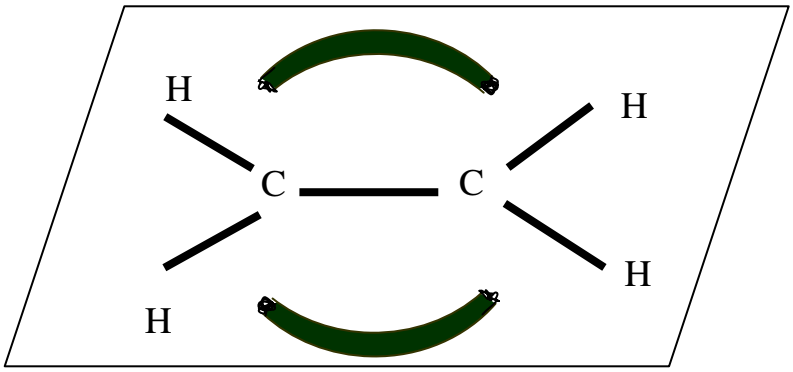

Fig. 2. 6. Overlap of 2p orbitals of carbon atom in ethylene to form a π-bond. Heavy lines show centers of σ bonds lying in the plane, and π bonds are perpendicular the plane.

To sum up, we have seen the formation of π-bonding and π^*-bonding MOs due to the overlap of p_z orbitals of the two neighboring carbon atoms in the sp^2 hybridization. In the case of polymers, where many monomers are coupled together, the π-bonding will become more delocalized and more atomic orbitals must be included in the over all MO description. The bonding orbitals will tend to cluster together into tightly packed groups with spacing between the energy levels being so small that we can treat it as a continous band of energy levels. Antibonding MOs also form a continuous band of energy levels. Therefore, we call the cluster of fully occupied bonding orbitals (π-bands) as valence band (VB) and the cluster of vacant antibonding orbitals (π^*-band) as conduction band (CB). The gap between these two completely filled and completely empty bands is called the band gap or energy gap (E_g).

2.3 Physics Of One-Dimensional Solids

Many properties of solids are described based on idealized model of crystal lattice. The model of high symmetry lattice such as a cube, a square, or a line of equidistant lattice points in three-or two - or one-dimensional crystal lattice, respectively, have significant role in understanding solids.

Polymers are macromolecules made from a number of repeating units, which are coupled together forming a chain. Thus, polymer crystals are one-dimensional solids and we need to understand the physics of one-dimensional solids.

A set of mechanical objects of equal masses separated by distance a and linearly connected by elastic springs having different force constants, or an array of a pair of unequal masses arranged linearly and connected by springs having the same force constant, can be used as a model for one-dimensional crystal. The restoring force is the bonding force. Disturbing the system by displacing an atom slightly from its equilibrium position develops waves called sound waves.

By inserting plane wave into equation of motion, one can drive the relation between angular frequency (ω) and wave vector (k), which is known as dispersion relation. The frequency of vibration of a given crystal is related to energy while the wave vector is related to the velocity. The dispersion relation of the system is depicted in the Fig.2.7 below.

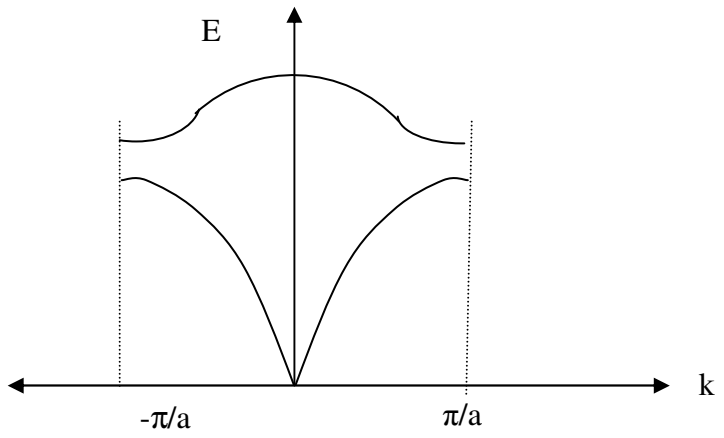

Fig. 2. 7. Dispersion relation of phonons in a crystal (linear diatomic lattice).

The classical "free" electron models gives a parabolic dispersion relation (see Fig 2.8 (a)) and successfully addresses the physics of electron transport in metallic solids, but fails to explain some properties of metals (e.g. specific heat capacity). On the other hand, nearly free electron model dispersion relation [16] revealed discontinuities at the boundary zones as shown in the

Fig. 2.8 (b). The first Brillouin zone is a reciprocal space repeat cell bounded by certain k values (e.g. $k = \pm \pi/a$). At the boundary, a single k value has two energy values. Energies between these values are not allowed and the difference of these values is the energy gap (E_g).

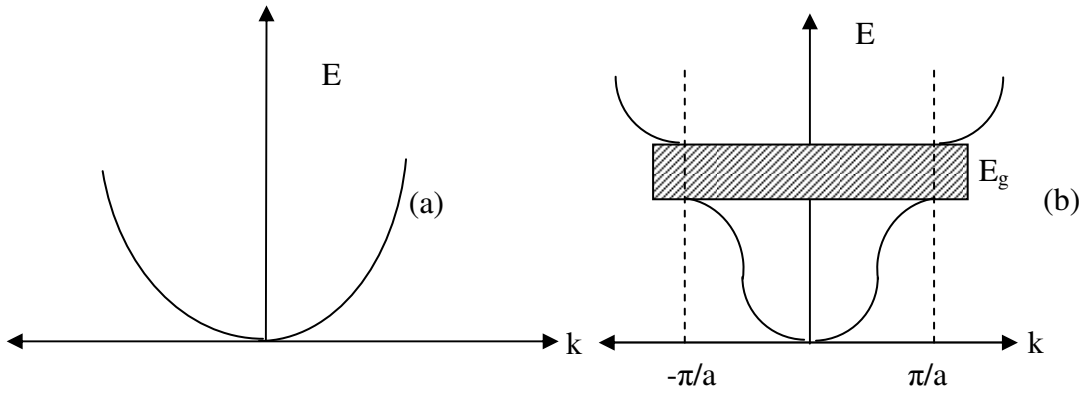

Fig. 2. 8. Dispersion relations for free electron (left), and nearly free electron (right) model.

2.4 Electron-Lattice Coupling, Peierls Transition

An important case of electron-lattice coupling is Peierls transition. In 1955, Peierls [17] showed that a monatomic metallic chain is unstable and will undergo a metal- to -insulator transition at low temperature.

Suppose that equidistant monatomic sodium atoms form a chain, see Fig. 2.9 (a). Although it is not possible to synthesize an isolated chain of such type, it is possible to calculate the electronic dispersion relation and electronic density of states of such system as depicted in the Fig. 2.9 b&c respectively.

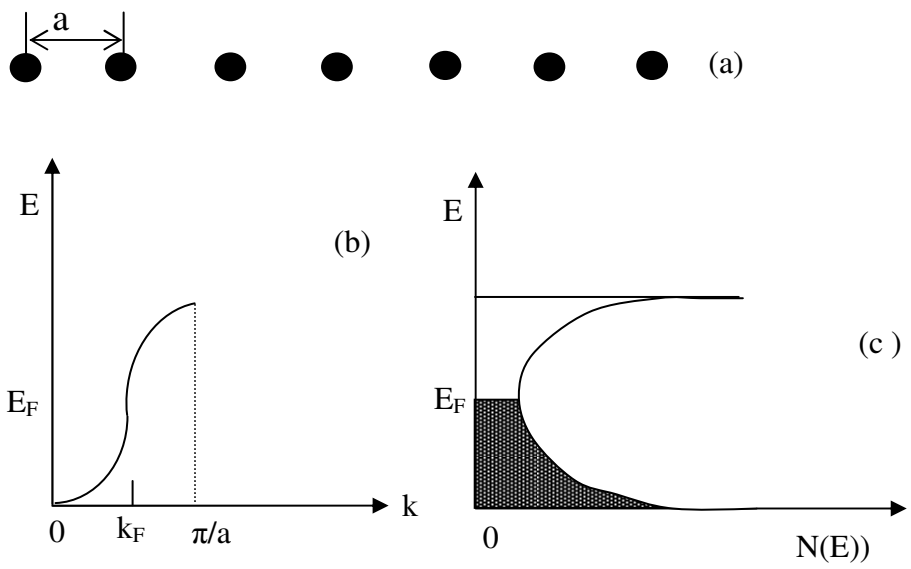

Fig. 2. 9. (a) Undistorted crystal lattice in 1-D, (b) its dispersion relation, and (c) its electronic DOS.

Each sodium atom contributes one electron to the conduction band. A single state can

accommodate two electron of spin up and spin down because of Pauli's exclusion principle. Therefore, the energy band is half filled. The band diagram (Fig. 2.9 (b)) reveals that the Fermi wave vector k_F and Fermi energy are half way between 0 and π/a and at the center of the band, respectively.

Again let's imagine that every other sodium atom is displaced by an amount δ, so that short distance $a- \delta$ and long distance $a + \delta$ alternate. The perturbed chain is still periodic, but with repeat distance 2a instead of a. Consequently, the reciprocal lattice changes from $2\pi/a$ to π/a. Clearly, the boundary of the first Brillouin zone changes from π/a to the Fermi wave vector $\pi/2a$. The former lattice (arrangement of atoms with period a) causes the electrons to have a gap at π/a, but the new lattice creates an additional gap at $\pi/2a$, thereby transforming the system from a metal with no gap at the Fermi level into a semiconductor (insulator) with a gap. All states below the gap are filled at absolute zero, but all states above are empty. The figure of perturbed arrangement of the system, and its dispersion relation and electronic DOS are depicted in the Fig.2.10 below.

Peierls, who studied this effect in 1955, postulated that a one-dimensional monatomic metal lattice with equidistant separation a would be energetically unstable against a periodic distortion.

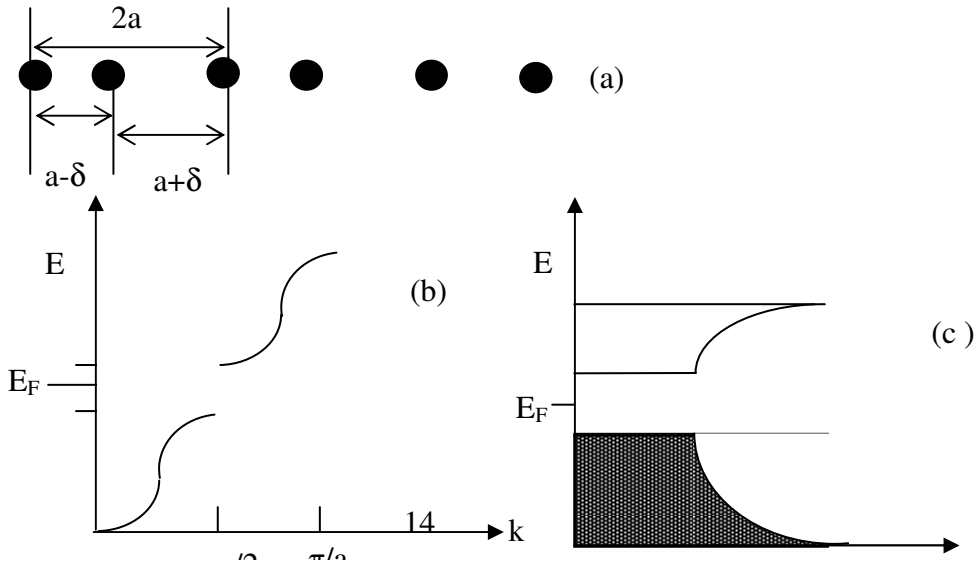

Fig. 2. 10. Peierls transition of a 1-D crystal lattice. Crystal lattice (upper), electronic DOS (lower right) and dispersion relation (lower left).

2.8 Peierls Distortion In Polyacetylene

Assume that simplified structure of polyacetylene as extended chain instead of zigzagged, with a bond angle of 180^0 instead of 120^0 prepared by dehydrogenation from polyethylene. Removing one hydrogen atom from each carbon atom leaves unbonded electron everywhere. Each $CH^{\cdot}$ radical has one delocalized electron, which has some similarity with an alkali atom, say Na, both have an extra electron. The poly $CH^{\cdot}$ chain in Fig. 2.11 (a) thus resembles the sodium chain in Fig. 2.9 (a).

The unbonded electrons of C-atoms, which are p-electrons, give rise to the metallic state in the same way that the s-electrons in alkali metals result in their metallic properties. The bonds of polyacetylene depicted in Fig.2.11 (a) are sort of one and half bond, which have the same length. Thus, band is half filled. However, Peierls showed that such type of metallic state is not stable and it undergoes through metallic to non-metallic state transition.

The p-electrons now become localized, thereby forming alternating double bonds. In other words, alternating single and double bonds will be formed. Double bonds are stronger than single bonds. Consequently, the bond lengths of double bonds are shorter than that of single

bonds. This difference in bond length of polyacetylene is similar to short $a-\delta$ and long $a+\delta$ lengths of the perturbed sodium atoms as in the Fig. 2.10 (a).

From theoretical point of view, a peierls distortion is a disorder- to- order phase transition in electronic systems. The non-metallic state of polyacetylene is called dimerized polyacetylene. Moreover, during dimerization process, the $CH^{\cdot}$ radicals become paired and distort the regular array of the lattice and hence double the elementary cell of the one-dimensional crystal lattice. Doubling of elementary cell in the real space corresponds to reducing the Brillouin zone by half in a reciprocal space.

Dimerization of undimerized polyacetylene introduces energy gap in dispersion relation and density of state. The structures of dimerized and undimerized polyacetylene with their respective dispersion relation are shown below in Fig 2.11.

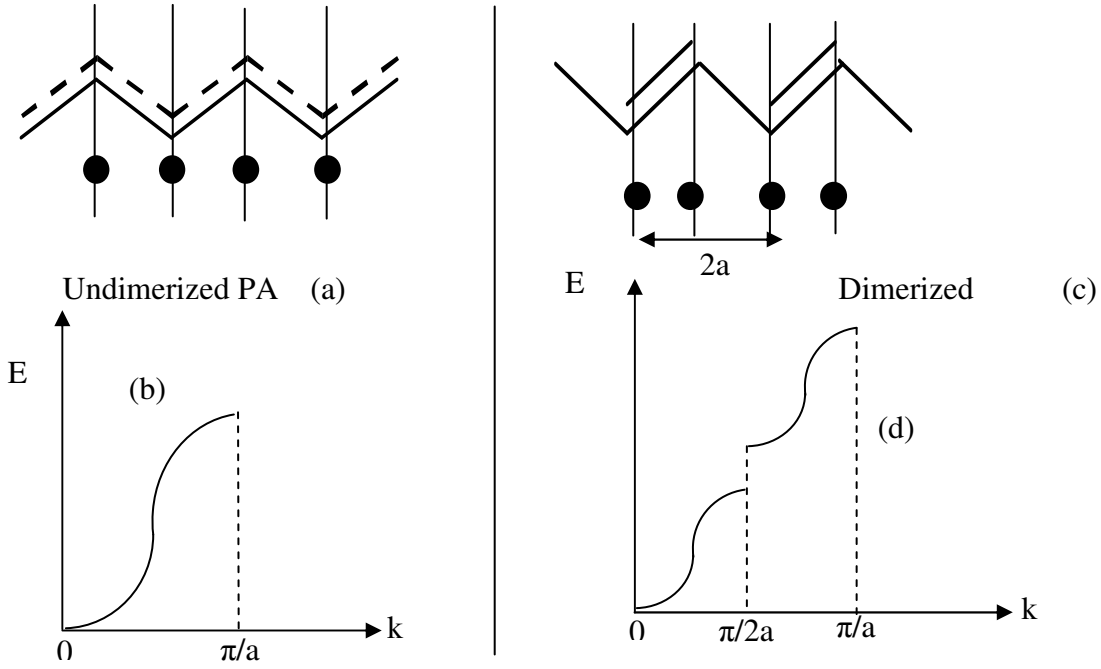

Fig. 2. 11. In peierls distortion of every second $CH^{\cdot}$ radical is moved through the same displacement, the real space unit cell width doubles to 2a and the corresponding width

of the reciprocal unit cell reduces to half, that is, $k_F = \pi/2a$. The source of the distortion is dimerization of the undimerized polyacetylene.

3. Elementary Excitations

The modern theory of condensed matter is based on the assumption of the existence of a stable ground and excited states of higher energy. Elementary excitations like phonons (lattice vibration or sound waves), magnons (spin waves), photons (electromagnetic waves), solitons (solitary or "water" waves), etc., are building block of a solid in the sense of motion as atoms, ions or molecules are the building blocks of a crystal in a sense of structure. In most cases the energy of excited state can be expressed as a sum of energies of elementary excitations. Elementary excitations, which are also called quasi-particles, exist in conjugated polymers. These are solitons, Polarons and bipolarons. In the following sections quasi-particles in conjugated polymers will be discussed.

3.1 Solitons

There are some ways to generate solitons in particular, polarons and bipolarons in general in

conjugated polymers. These are doping (oxidation or reduction) of polymers, during synthesis of polymers, and photogeneration [15]. Solitons in polyacetylene are most extensively studied [17-27] and serve as a model for understanding the electronic and physical properties of conducting polymers.

The trans-polyacetylene having two fold degenerate ground states, one with positive slop, phase A, and the other with negative slop, phase B, are shown in the Fig. 3.1 below.

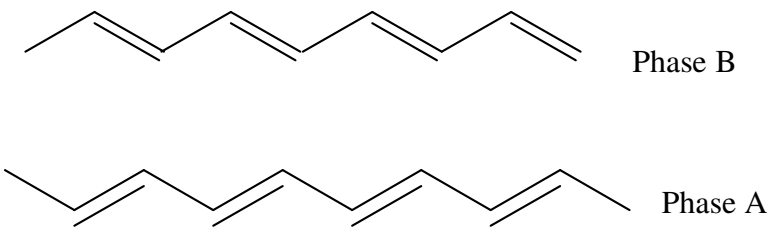

Fig. 3. 1. Ground state degeneracy of dimerized trans-polyacetylene. The ground state energy of phase A is the same as that of phase B.

If the undimerized PA undergoes peierls transition to the dimerized one and dimerization starts simultaneously at both ends of the polymer chain, then there is a 50% probability of a misfit (two single bonds meet) formation as the process propagates to the center, see Fig. 3.2 below.

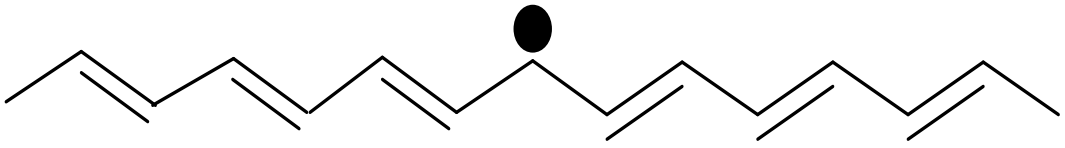

Fig. 3. 2. A domain wall (soliton) separating trans-PA chain into domains similar to

phase A (right) and phase B (left) as in the above figure.

The strict alternation of single and double bonds (conjugation) (Fig. 3.2) is interrupted and there is formation of domain wall that separates two phases of opposite orientation and identical energy. The reason for the gap in the energy band structure of conjugating polymers is the bond alternation. However, the formation of a misfit leads to an electronic state in the gap, and the state under ideal circumstances is exactly at the midgap [28]. At the misfit atomic orbitals don't know whether they should form the π-bonding or the π^*-antibonding and because of symmetry reason they form a midgap state. This conjugational defect is called soliton. Soliton can be neutral (q = 0), positive (q = e), or negative (q = -e) with spin 1/2, 0, and 0, respectively.

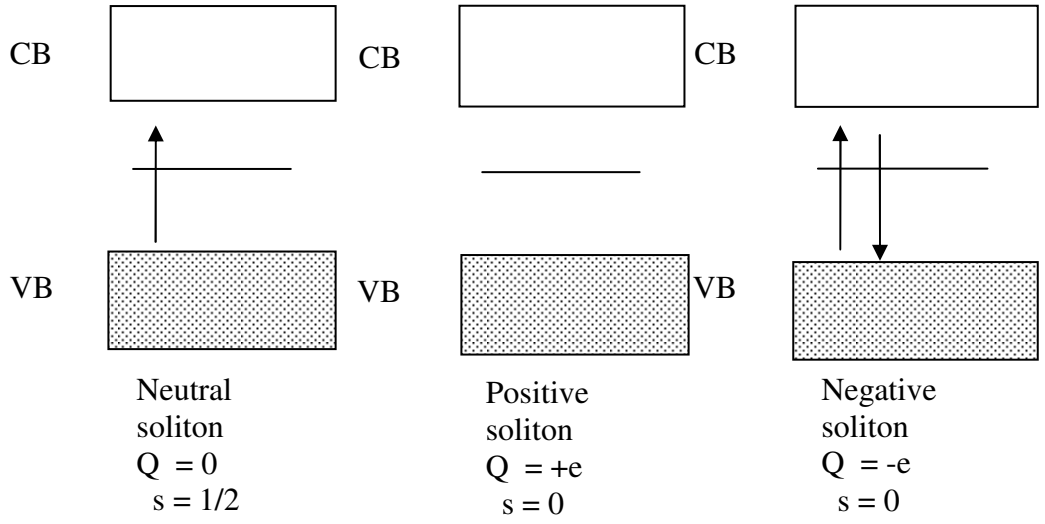

Fig. 3. 3. Schematics of the band diagram of polyacetylene with soliton.

Charged solitons don't carry spin, while neutral solitons have spin s = 1/2.

Doping (oxidation or reduction) is another way of producing conjugational defects. Solitons produced in doped polyacetylene are believed to be delocalized over about 12 CH units with

maximum charge density next to the dopant concentration. The bonds closer to the defect show less amount of bond alternation than the bonds away from the center. Soliton formation results in the creation of new localized state that appears in the middle of the energy gap. Therefore, as dopant concentration increases more states in the gap will be formed. At higher doping levels, the charged solitons interact with each other to form a soliton band with its upper and lower soliton band edges merge with the conduction and valence band to create true metallic conductivity.

3.2 Polarons And Bipolarons

Polarons in an ionic crystal are used to represent the effect of a moving electron in ionic crystal, that is, lattice distortion and the electron itself. A moving electron attracts positive ions and repels negative ions. Therefore, it creates polarization field. However, polaron in conducting polymer is used to denote a localized electron states with accompanying lattice distortion. It is described as bounded state of soliton and antisoliton. Unlike polyacetylene, which has both degenerate (trans-PA) and non-degenerate (cis-PA) ground states, all other conjugated polymers have non-degenerate ground state. As an example, the Fig. 3.4 below shows the two forms (aromatic and quinoidal) of a non-degenerate polythiophene.

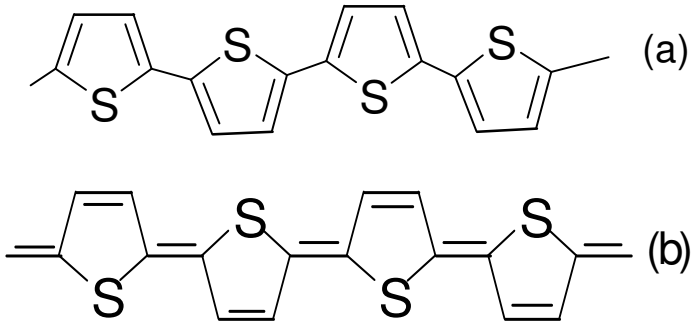

Fig. 3. 4. Two non-degenerate forms of polythiophene

(a) aromatic and (b) quinoidal form of polythiophene.

When the aromatic state of polythiophene is bonded to the quinoidal state, a soliton will be formed, see Fig. 3.5 below. Since the aromatic state is lower in energy (ground state) and quinoidal state is higher in energy, the soliton will be driven out to the end as the higher-energy quinoidal rings change to the lower energy aromatic rings. Hence, solitons in non-degenerate polymers are unstable.

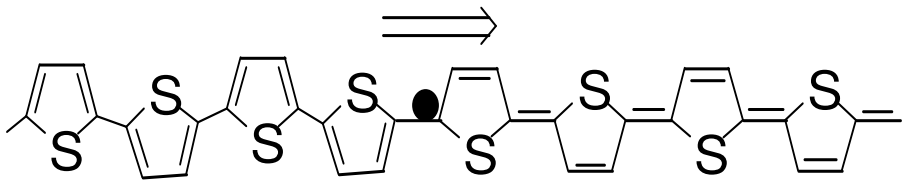

Fig. 3. 5. The energy of the aromatic configuration (ground state) is less than the quinoidal (excited) state energy. Hence, the lattice forces drives solitons in direction of the arrow.

If an electron is removed by breaking a double bond connecting two quinoidal rings (Fig. 3.5), then bonded-double defect called polaron will be formed. Further removal of an electron from the already oxidized polymer containing the polaron results in the generation of a doubly charged state termed as bipolaron. The bounded-double defects, polaron and bipolaron are shown in Fig 3.6 (a) and (b) respectively.

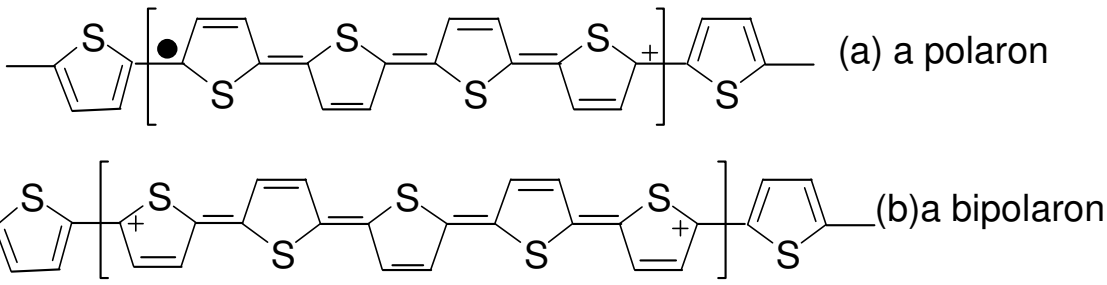

Fig. 3. 6. Formation of a polaron and bipolaron in polythiophene.

The neutral non-degenerate conjugated polymers have completely filled valence and completely empty conduction bands separated by a band gap. Generation of a polaron or a bipolaron creates two localized electronic states, which are located symmetrically in the band gap. For instance, bipolaron states are 0.5eV away from band edges for PTOPT doped with $NOPF_6$ [29]. The energy band structures of the polaron and bipolaron are shown below.

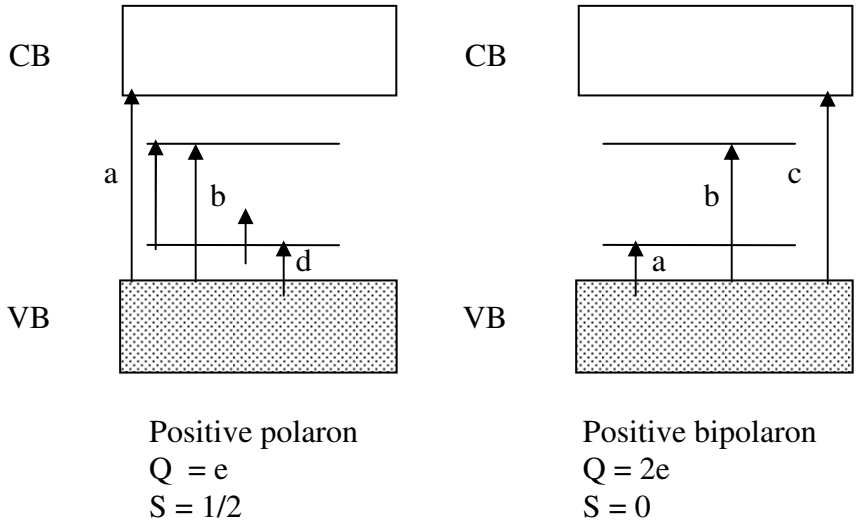

Fig. 3. 7. The band diagram of a hole polaron (left) and a hole bipolaron (right) with possible optical transition.

Similar to the formation of solitonic band by heavily doping, the discrete localized polaronic and bipolaronic states in the band gap can also be changed to a continuous bipolaronic band. For a heavily doped polymer, it is conceivable that the upper and lower bipolaronic band edges will merge with conduction and valence bands respectively, to produce partially filled band, and metallic like conductivity will be achieved.

Optical absorption spectroscopy provides experimental evidence for the existence of the

electronic states in band gap of the conjugated polymers. As an example, the optical absorption of PTOPT in its neutral and doped state is depicted in the Fig. 3.8 below [29], where "a" refers to transition from valance bond to the lower state, "b" represents transition from valance band to the upper state, and "c" represents inter band transition.

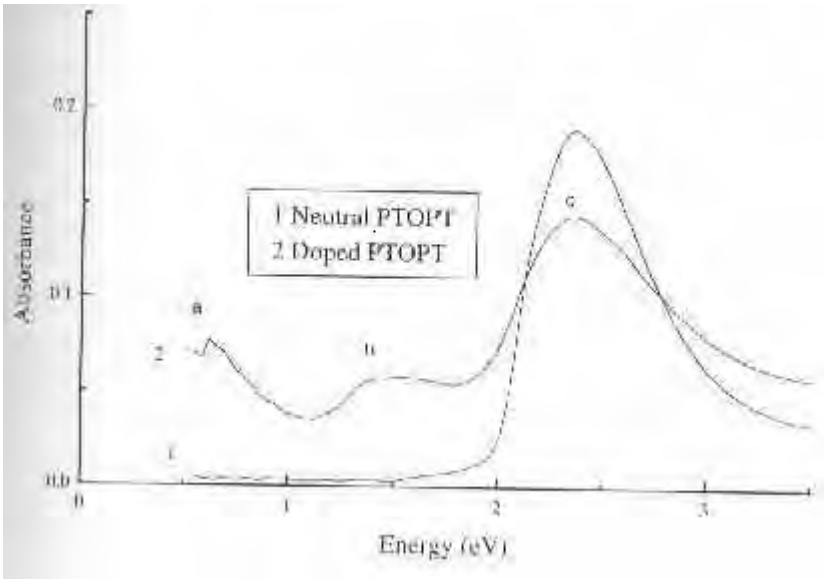

Fig. 3. 8. Absorption spectroscopy of neutral and doped PTOPT

3.3 Charge Transport Mechanism And Electrical Conductivity

The conduction mechanism of organic semiconductors does not follow the same theory as that of crystalline inorganic semiconductors and metals, where conduction in these materials are due to separate and free charge carriers transport. Much research has been carried out on conduction mechanism of polyhetrocycles such as polypyrole [30], polyacetylene [31], and poly (3-hexylthiophene) [32].

Although the precise mechanism is not yet fully understood, solitons, polarons, and bipolarons are believed to be the main source of charge transport. The complex structure and morphological forms may directly affect the transport of charge carriers. It also affects conductivity of conducting polymers. However, the conductivity of these materials can be varied 12 orders of magnitude through doping [17].

Temperature dependence of conductivity of materials shows different relation or dependence. For instance, conductivity of metals increases with decreasing temperature while the amorphous and crystalline inorganic semiconductor conductivity decreases exponentially with cooling. Moreover, the theoretical and experimental work showed temperature dependence of conductivity of conducting polymers and it decreases with cooling, but it is slower than exponentially dependence.

Doping enhances conductivity and affects the temperature dependence of conductivity. At low level of doping of polyacetylene with iodine shows a steep slope temperature dependence of conductivity while high level doping has flattened curves [33]. Thus, a single model could not explain the charge transport mechanism of conducting polymers.

Lack of periodicity of lattice of conducting polymers leads to use the concept of conductivity developed for amorphous materials [17]. There is no E(k) relation (dispersion relation) like crystalline semiconductors. However, it is possible to plot the density of state against energy, see Fig.3.9.

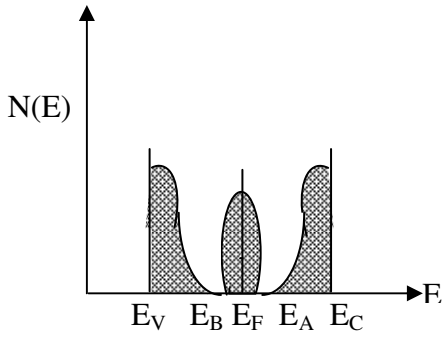

Fig. 3. 9. The density of state for non-crystalline solids near a gap. E_V and E_C are boundaries between localized and extended states called the "mobility edges", and E_A and E_B are the band edges.

Though conduction mechanism exits due to thermal excitations to extended states, there is also another mechanism called hopping process (an abbreviation for " phonon assisted quantum mechanical tunneling") between the localized states in the gap. Hopping conductivity assumes the random distribution of localized states. The variable range hopping (VRH), the main dominant process in lightly doped and undoped conducting polymers, was suggested by Mott [17]. Mott's VRH dc conductivity is given by

$$\sigma = \sigma_o \exp\left\{-\left(\frac{T_o}{T}\right)^{\gamma}\right\}, \qquad 3.1$$

where σ_o and T_o are experimentally determined fitting parameters, γ depends on the dimensionality of hopping process and given by $\gamma = \frac{1}{1+d}$, for d = 1,2,3, γ will be 1/2, 1/3, 1/4 respectively. For γ =1/4 equation (3.1) reduces to Mott's famous $T^{-1/4}$ law at low temperature [34]. The variable range hopping has been applicable to poly (3-hexylthiophe) [32], polyacetylene [17], and polypyrole [35]. However, this model couldn't be applied for highly doped conducting polymers having localized gap states, which are not random and their defects cluster together.

Another model introduced by Sheng [36] assumes highly doped polymers as metallic islands in an insulating matrix and conductivity can be described by fluctuation-induced tunneling. It is given by

$$\sigma = \sigma_o \exp\left(-\frac{T_o}{T_1 + T}\right), \qquad 3.2$$

where σ_o, T_o and T_1 are parameters which depend on the size of metallic islands and geometry of potential barrier between the islands.

(a) For $T \ll T_1$, equation 3.2 reduces to constant conductivity of the polymer given by

$$\sigma = \sigma_o \exp\left(\frac{-T_o}{T_1}\right), \text{ and} \qquad 3.3$$

(b) For $T \gg T_1$,

$$\sigma = \sigma_o \exp\left(\frac{-T_o}{T}\right). \qquad 3.4$$

4. Electrical Properties Of Metal-Semiconductor (Polymer) Contact

4.1 Metal-Semiconductor Contact

Depending on the majority charge carrier of the semiconductor, we can classify semiconductor as p-type (majority carriers are holes), n-type (majority carriers are electrons) and intrinsic semiconductors (both carrier concentration are equal). When they make intimate contact with a metal, a Schottky barrier may be formed.

To see a formation of a Schottky barrier, suppose that both metal and semiconductor, which are electrically neutral when separated from each other and have no surface stases, make an ideal intimate contact to each other. a) Consider first the n-type semiconductor of low work function (ϕ_s) as compaired to the work function of the metal (ϕ_m). The energy band-diagram when they are separated from each other is shown in Fig 4.1 below [10].

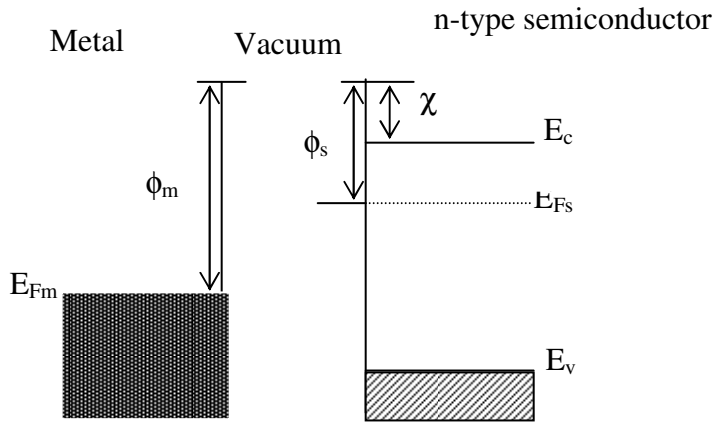

Fig. 4. 1. Band diagram of metal and n-type semiconductor before contact for $\phi_m > \phi_s$.

When the semiconductor is brought in contact with the metal, electrons will flow from the semiconductor to the metal across the interface to establish equilibrium. During this process, some part of the semiconductor will be depleted of charges. Thus an electric field directed from semiconductor to metal will be formed. At equilibrium, the Fermi levels of the metal and the semiconductor attain same value and the energy-band diagram will no longer be as in Fig. 4.1. The flat conduction band and valance band bend upward in the semiconductor, as shown in Fig. 4.2.

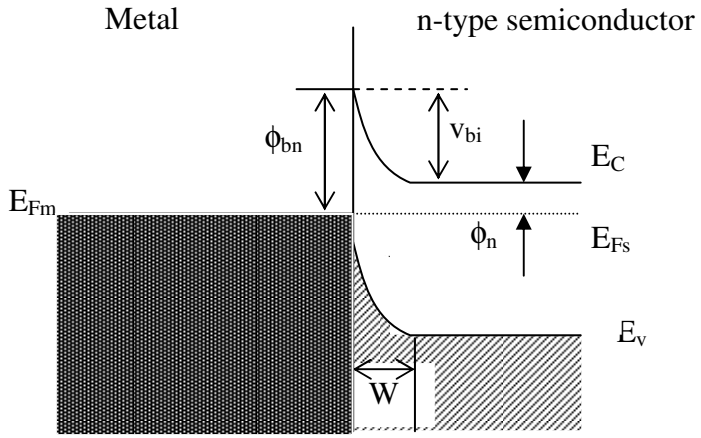

Fig. 4. 2. The energy band diagram metal-semiconductor (n-type) contact for $\phi_m > \phi_s$.

Clearly, we can see from Fig. 4.2 the formation of Schottky barrier with barrier height ϕ_{bn} and depletion width W. If positive voltage is applied to the metal, barrier height for electrons flowing from the semiconductor to the metal will decrease and barrier height for electrons flowing from metal to semiconductor is the same. This bias voltage is known as forward bias. If we apply positive voltage to the semiconductor, the barrier for electrons moving from the semiconductor to the metal will increase and barrier for electrons moving from metal to

semiconductor will remain the same. This applied bias is called reverse bias. Thus, a rectifying junction is formed.

The work function of a metal (ϕ_m) is the amount of energy required to raise an electron from the Fermi level to a state of rest outside the surface of the metal (so-called vacuum level) and the work function of a semiconductor (ϕ_s) is the difference between the Fermi level and vacuum level [10]. In the ideal contact (when there are no surface states, interband states and no interfacial layer), the quantity $q(\chi + \phi_n)$ is $q\phi_s$, where $q\chi$ is electron affinity measured from the bottom of the conduction band E_c to the vacuum level, and $q\phi_n$ is the difference between E_c and Fermi level. Thus, potential barrier for electrons in conduction band of the semiconductor trying to move into the metal or barrier height of semiconductor is given by

$$v_{bi} = \phi_{bn} - \phi_n . \qquad 4.1$$

Secondly, if the work function of the metal is less than that of an n-type semiconductor, electrons shall be transported from the metal to the semiconductor leaving negative charge on the surface of the metal that is in contact with the semiconductor. The band-diagram is shown below in Fig. 4.3. Whether we apply positive voltage or negative voltage to the metal, electrons can flow in both directions, which leads to the increase of its conductivity. In such case the contact is ohmic.

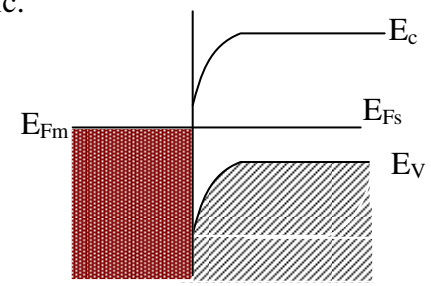

Fig. 4. 3. Band diagram of metal-semiconductor (n-type) contact for $\phi_m < \phi_s$.

b) The second case is when a p-type semiconductor is in intimate contact with a metal. If ϕ_m

$>\phi_s$, we obtain the band diagram shown in Fig. 4.4 (a) which represents ohmic contact. But, the case of p-type semiconductor for which ϕ_s exceeds ϕ_m, is analogous to the n-type of $\phi_m > \phi_s$ case discussed above, and there is formation of rectifying junction, see as Fig. 4.4.

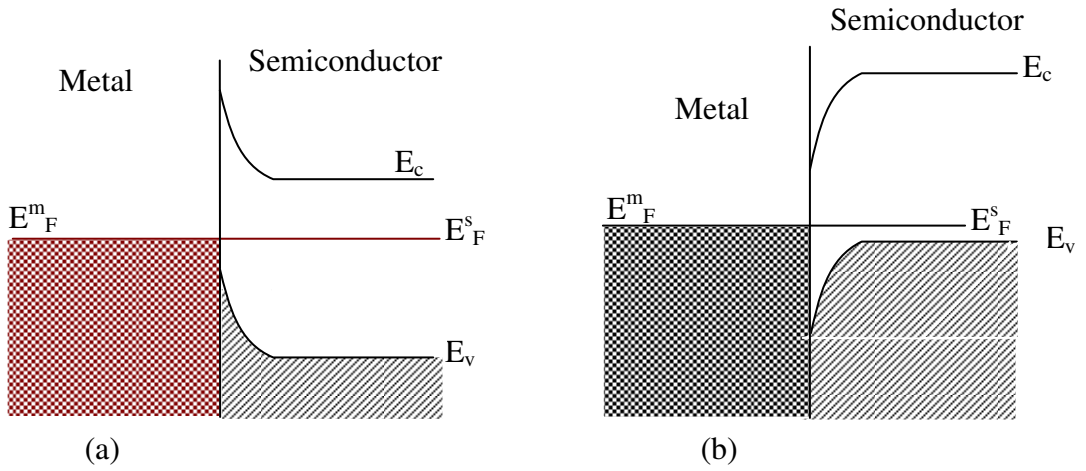

Fig. 4. 4. The energy band diagram of metal-semiconductor (p-type) for (a) $\phi_m > \phi_s$, which is ohmic and (b) $\phi_m < \phi_s$, which is a rectifying contact.

4.2 Current- Voltage Characteristics

The current transport- process for metal- semiconductor contacts is mainly due to majority carriers. We have seen before the formation of a Schottky barrier but did not mention about the ways of current transport across the junction that may affect the J-V relationship. Generally, there are various ways in which electrons can be transported across a metal-semiconductor junction under the forward bias. These processes for n-type semiconductor are shown below. But, the inverse processes occur under reverse bias [37]. These processes are:

(a) Emission of electrons from the semiconductor over the top of the barrier in to the

metal;

(b) Quantum-mechanical tunneling through the barrier;

(c) Recombination in the space-charge region; and

(d) Recombination in the neutral region ('hole injection').

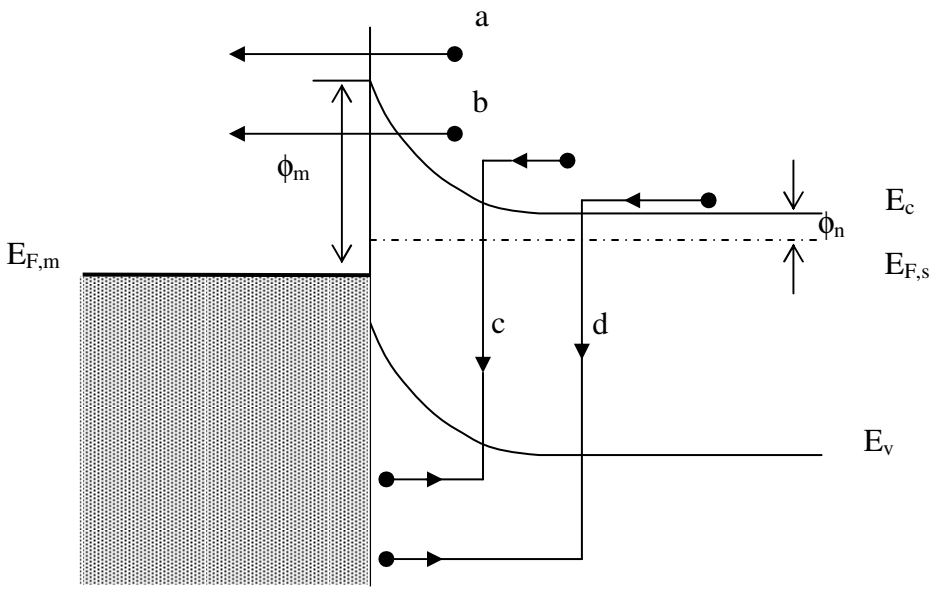

Fig. 4. 5. Four basic carrier transport processes under forward bias Schottky barrier diode

A basic transport process in rectifying Schottky diode of MS contact is the thermionic emission process, which is process (a) as shown in Fig. 4.5 above. The assumption of Bethe's thermionic emission theory, which is the current limiting process, is the actual transfer of electrons across the interface between the semiconductor and the metal over the barrier. Moreover, the barrier height is much larger than kT ($e\phi_{bn} >> KT$). It is possible to produce practical Schottky diode having J-V characteristics governed by thermionic emission and it is

given by

$$J = J_o\left[\exp\left(\frac{qV}{nkT}\right)-1\right], \qquad 4.2$$

where V is applied voltage, q the electronic charge, k Boltzman factor, T absolute temperature, n ideality factor, and Jo the saturation current density given by

$$J_o = A^{**}T^2\exp\left(\frac{-q\phi_b}{KT}\right), \qquad 4.3$$

where A^{**} is the modified Richardson constant and $120A/cm^2k^2$ [23,24] for an electron in free space, ϕ_b is barrier height. Simply by observing thermionic emission equation, we see that there are three cases:

1. If $J >> J_o$, the barrier effectively blocks the current for reverse bias and allows current for forward bias. And hence the diode rectifies.

2. If $J << J_O$, current can pass in the both direction (for forward bias and reverse bias) and the contact is ohmic.

3. If $J \sim J_o$ (when the saturation current density is approximately same as the current), J-V curve will be neither rectifying nor ohmic.

4.3 Capacitance-Voltage Characteristics

An independent way of determining the barrier height of Schottky diode is the measurement of capacitance at reverse bias voltage. By considering ideal Schottky diode (without any interfacial layer) and the semiconductor, which has a uniform donor concentration, we can write the differential capacitance of the junction as the function of reverse bias and it is given by

$$\frac{C}{A_s} = \left[\left(\frac{q\varepsilon_s N_d}{2} \right)^{1/2} \left(\phi_b - \phi_n - V - \frac{KT}{q} \right)^{1/2} \right], \qquad 4.4$$

where A_s is the cross-sectional area of the device, ε_s the dielectric constant of the semiconductor, N_d the (homogeneous) dopant density, V the applied voltage, kT/q the thermal energy expressed in volts and ϕ_b, ϕ_n are shown in Fig. 4.2.

By rearranging equation (4.4):

$$\frac{1}{C^2} = \frac{2}{qA_s\varepsilon_s N_d} \left[\phi_b - \phi_n - V - \frac{KT}{q} \right]. \qquad 4.5$$

From this equation, we can see that a plot of $1/C^2$ against voltage V should be a straight line. If the dielectric constant of the semiconductor is known, dopant concentration (density) can be calculated from the linear slope of the curve. The x-intercept of this line is $-\left(\phi_b - \phi_n - \frac{KT}{q} \right)$.

By calculating the potential ϕ_n and knowing the x-intercept from the plot immediately gives barrier height ϕ_b. The x-intercept of the line is the built-in voltage Vbi ($=\phi_{bn}-\phi_n$). Moreover, depletion width at zero-bias can be given by

$$w = \sqrt{\frac{2\varepsilon_o\varepsilon_r v_{bi}}{qN_d}}\,. \qquad 4.6$$

The above way of determining parameters works if and only if the MS contact is an ideal contact, that is, no interfacial layer and no inter-gap states or surface states. In the other way round, some conjugated polymer/metal junction forms a thin insulating layer up on the depositing of low work function metal such as aluminium [38]. This is a metal-insulator-semiconductor (MIS) contact that has many uses in device physics.

A Schottky diode behaves in the same way as a parallel-plate capacitor. Therefore, the

capacitance of the capacitor is given by

$$C = \frac{\varepsilon_o \varepsilon_r A_s}{w}, \qquad 4.7$$

where ε_o is permitivity of free space, ε_r is the relative permitivity of the semiconductor (ε_r is 3 for polymers [39]), and depletion width W is then given by

$$w = \frac{\varepsilon_o \varepsilon_r}{\left(C / A_s \right)}. \qquad 4.8$$

4.4 Impedance Spectroscopy

Impedance spectroscopy is a relatively new and powerful method of characterizing many of the electrical properties of materials and their interfaces with electronically conducting electrodes. It may be used to investigate the dynamics of bound or mobile charges in the bulk or interfacial regions of any kind of solid or liquid medium that is ionic, semiconducting, mixed electronic-ionic, and even insulating [40].

The general approach of impedance spectroscopy experiment is to apply an electrical stimulus to the electrode and observe the response. There are three different types of electrical stimuli, which are used in impedance spectroscopy. The first and the second are applying a step function voltage ($v(t) = 0$ for t < 0, $v(t) = V_o$ for t >0) and a signal voltage $v(t)$ composed of random noise to the system and measuring current respectively. These approaches have advantages and limitations. The third approach, the most common and the standard one, is to measure impedance directly in the frequency domain by applying a single- frequency voltage to the interface (system) and measuring phase shift and amplitude, or real and imaginary parts of resulting current at that frequency.

Impedance, more general concept than resistance, was first introduced by Oiver Heaviside in the 1880s and was soon after developed interms of vector diagram (phases) and complex representation by A.E.Kennelly and especially C.P. Steinmetz. Its conventional definition is $Z(\omega) = {v(t)}/{i(t)}$, where $v(t)$ is the applied monochromatic signal $v(t) = v_m(t)\sin(\omega t)$, with $\omega = 2\pi f$, to the device under test (DUT) and i(t) resulting steady state current $i(t) = I_m \sin(\omega t + \theta)$. Here θ is the phase difference between the voltage and current. The magnitude and direction of a planar vector in a right-hand orthogonal system of axes can be expressed by the vector sum of the components Z' and Z'' along the axes, that is, by the complex number Z = Z' + jZ''. The imaginary number $j \equiv \sqrt{-1} \equiv \exp\left(\frac{j\pi}{2}\right)$ indicates an anticlockwise rotation by π/2 relative to the x-axis, and imaginary part Z'' is along y-axis.

Experimentally obtained data for a given electrode-material system may be analyzed by modeling an equivalent circuit composed of ideal resistor and capacitor. There are some reports used this method [41-43].

Consider a parallel RC circuit model shown in Fig. 4.6

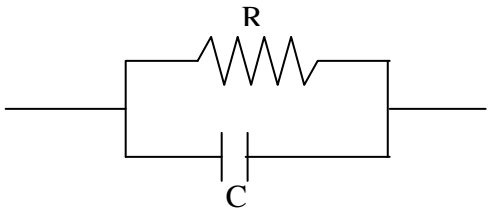

Fig. 4. 6. Parallel RC circuit.

The impedance of the parallel RC circuit is given by:

$$Z = \frac{R}{1 + j\omega RC} = \frac{R}{1 + (\omega CR)^2} - j\frac{\omega CR^2}{1 + (\omega CR)^2}. \qquad 4.9$$

The real and imaginary components of impedance are given by:

$$Z' = \frac{R}{1 + (\omega CR)^2}, \qquad 4.10$$

and

$$Z'' = \frac{\omega CR^2}{1 + (\omega CR)^2}. \qquad 4.11$$

The ideal Cole-Cole plot of parallel RC circuit will be a semicircle, whose center lies on the real axis, see Fig. 4.7.

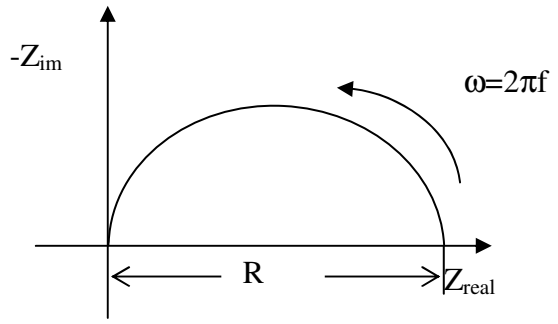

Fig. 4. 7. Cole-Cole plot of parallel RC circuit.

Suppose that a contact resistance R_c is connected in series with the parallel RC circuit as shown in the Fig. 4.8 below. Then the impedance is given by:

$$Z = R_c + \frac{R}{1 + j\omega CR}. \qquad 4.12$$

and its Cole-Cole plot is shown in Fig 4.8

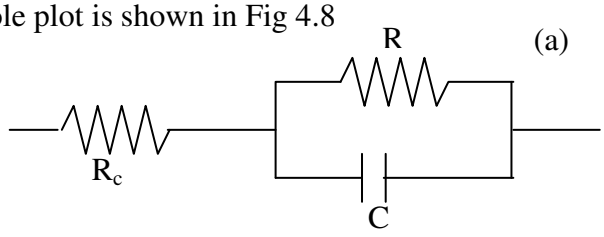

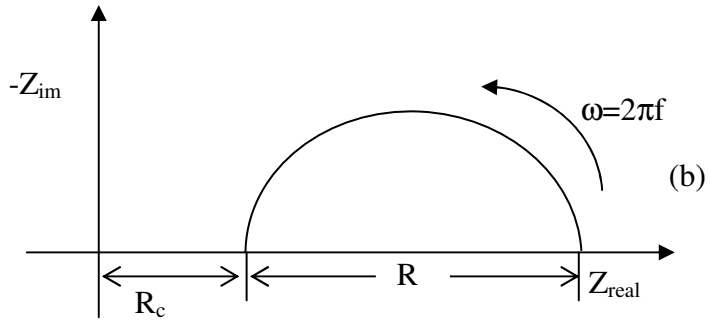

Fig. 4. 8. Circuit diagram for a contact resistance R_c in series with parallel RC circuit (a) and its Cole-Cole plot (b).

The circuit model shown in the Fig 4.8 is an equivalent circuit model for a metal-semiconductor junction in which the depletion region accounts for the observed capacitance and resistance, where as the contact resistance accounts conduction along the evaporated electrode.

A metal-insulator-semiconductor (MIS) device can be modeled using an equivalent circuit shown in Fig. 4.9. The complex impedance of

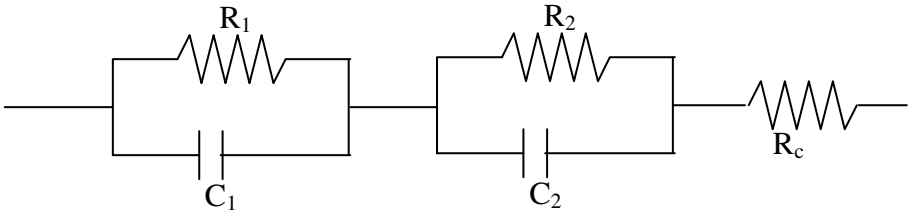

Fig. 4. 9. An equivalent circuit as modeled for an MIS device.

the equivalent circuit is given by:

$$Z = R_c + \frac{R_1}{1 + j\omega R_1 C_1} + \frac{R_2}{1 + j\omega R_2 C_2}, \qquad 4.13$$

where R_c is the series resistance that accounts for the conduction along the evaporated metal electrode, R_1 and C_1 represent resistance and capacitance of the insulating layer, and R_2 and C_2 stand for the depletion region. The Cole-Cole plot for such model is shown in Fig. 4.10.

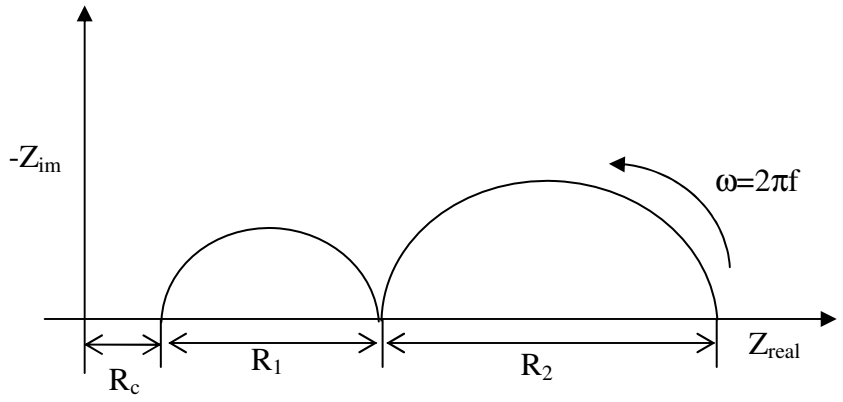

Fig. 4. 10. Idealized Cole-Cole plots for the circuit shown in Fig. 4.9.

5 Experimental Details

5.1 Absorption Spectrum

A 5mg solid polymer was measured by a sensitive balance and dissolved in 1ml chloroform. This solution was used for the absorption spectroscopy, current-voltage, and impedance spectroscopy measurement.

The solution was spin coated for optical absorption measurement on clean glass giving high quality reddish yellow solid film of about 200-300nm thicknesses. To produce such a thin film of the polymer, the spin coater is made to rotate at about 600rpm. The absorption spectroscopy was obtained using the Perkin Elmer λ19 UV/VIS/NIR spectrometer by putting the thin film of polymer on glass in the sample holder. This instrument is interfaced with computer having Ultra-Violent computer spectroscopy software (UVCSS).

5.2 Current-Voltage Measurement

A glass, which is pre-coated with transparent conducting indium tin oxide (ITO), was cut in to 3cmx3cm ($9cm^2$) piece. About two third of the piece was covered with photoresist, and immersing into a mixture of concentrated HCl, HNO_3 and H_2O of 48:4:48 by volume to etch the uncovered part of the ITO from the substrate. Therefore, the piece, which was as in the Fig. 5.1 (a), after etching changed to the situation as shown in Fig. 5.1 (b). The etched part helps for electrical contacts to the almunium layer, which will be deposited latter. The photoresist was then removed using acetone and the whole surface was washed with distilled water and methanol, and rinsed with ethanol.

The solution of polymer prepared as discussed above was spin coated on the clean ITO/glass substrate. For electrical contact on both sides of etched part (pure glass) and ITO part, the polymer was cleaned by chlorofo rm. The

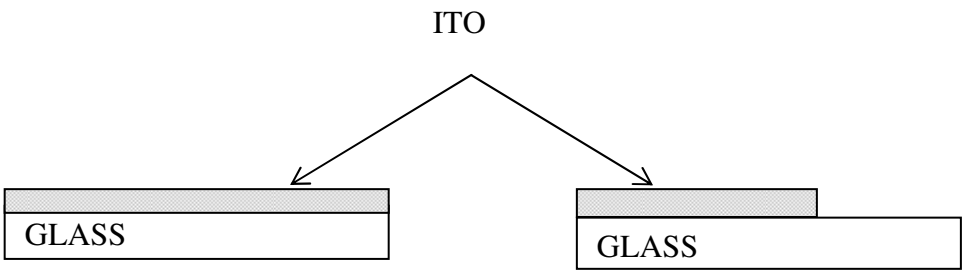

(a) (b)

structure is shown in the Fig. 5.1 (c) below.

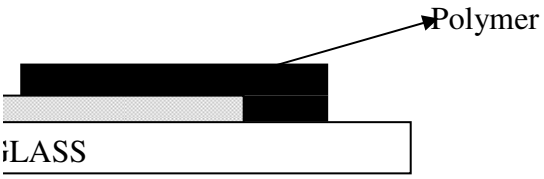

(c)

Fig. 5. 1. preliminary steps in preparing the device.

The final structure of the sample, Al/the polymer/ITO-glass, was obtained by evaporating aluminum on the polymer /ITO-glass substrate using Edwards Auto 306 vacuum evaporator. The thickness of aluminum was approximately 600nm. At the inset of evaporation the pressure was $3x10^{-5}$ mbar. The sandwich structure of Al/the polymer/ITO-glass is depicted as in Fig 5.2 (b)

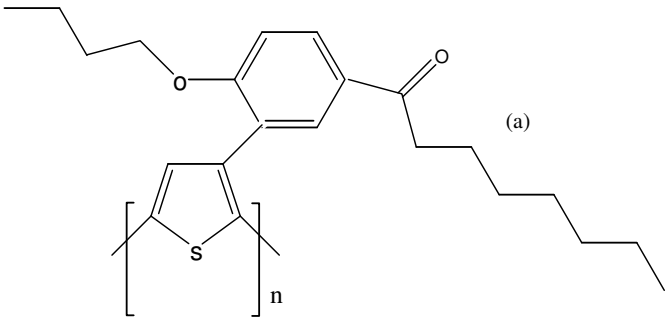

(a)

Poly[3-(2'-butyloxy-5'-(1'''-oxooctyl)phenyl)thiophene)

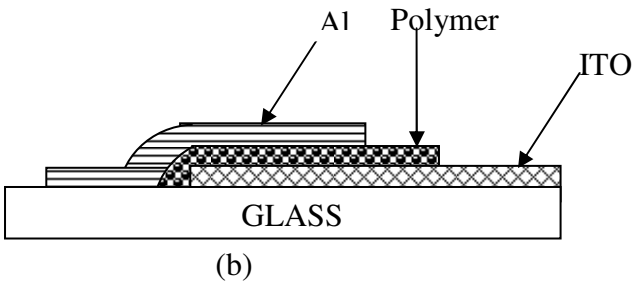

(b)

Fig. 5. 2. Chemical structure of poly[3-(2'-butyloxy-5'-(1'''-oxooctyl)phenyl)thiophene] and the sandwich Al/the polymer/ITO-glass diode.

The current-voltage measurement of the sample in Fig 5.2 (b) was done by connecting the aluminum electrode to the negative terminal of the voltage source for a forward bias. The instrument used for the I-V measurement was HP4140B PA meter (DC voltage source) interfaced with HP 16055A text fixture for sample holder in dark, at room temperature in dry air during the whole measurement.

5.3 Complex Impedance Measurement

The instrument, HP4192A low frequency impedance analyzer together with HP 16047-text fixture, was used for measuring complex impedance spectroscopy. The impedance spectroscopy of a sandwich structure of Al/polymer/ITO was characterized by measuring the complex impedance (real and imaginary parts) at applied bias voltages of 6v, 5v, -5v, and -6v. The frequency was scanned between 30Hz and 100kHz for each bias voltage. A sinusoidal oscillation voltage of V_{rms}=10mV was applied for every bias voltages.

6 Results And Discussion

6.1 Absorption Spectrum

It is well known that absorption spectrum reveals the presence of intergap states and their optical transition in addition to the π-π^* optical transition (or interband transition). Hence, one can determine the energy gap from the absorption spectrum. The absorption spectra in the wavelength range between 300nm and 700nm of poly [3-(2'-butyloxy-5'-(1'''-oxooctyl) phenyl) thiophene] is depicted in Fig 6.2 below. It is obvious from the plot that the polymer absorbs light in the visible range. After having the wavelength at which the onset occurs from the curve (λ = 617 nm) and by applying the relation $E_g = \frac{hc}{\lambda}$, the band gap of the polymer is calculated to be 2eV. Thus, the polymer energy gap falls in the range between 0.7 eV and

3 eV and assures us that the polymer is one among semiconducting organic polymers.

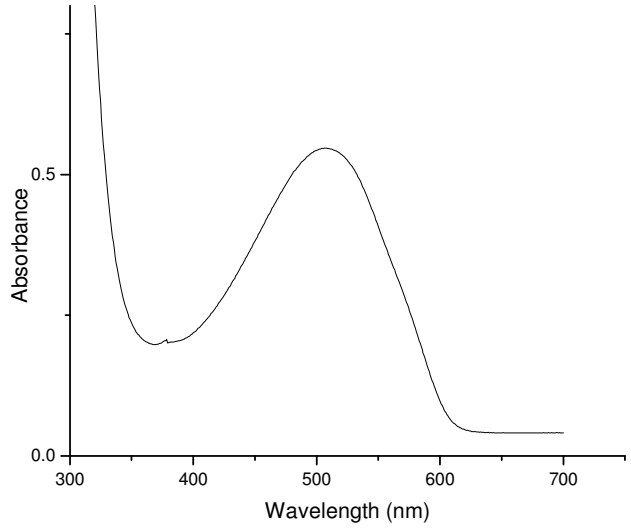

Fig. 6. 1. Absorption spectrum of poly[3-(2'-butloxy-5'-(1'''-oxooctyl)phenyl)thiophene].

6.2 Current Density-Voltage Characteristics

The dark current density-voltage characteristics of the Al/polymer/ITO sandwich type devise at room temperature is depicted in Fig. 5.2. Clearly, the J-V curve is asymmetric and non-ohmic. From the curve, the device blocks current in the reverse bias (negative voltages) and allows current in the forward bias (positive voltages) and hence it manifests rectifying behavior. The rectification ratio between forward bias current and reverse current at +/- 5.6V is obtained approximately $\frac{J_F}{J_R} = 1761.$

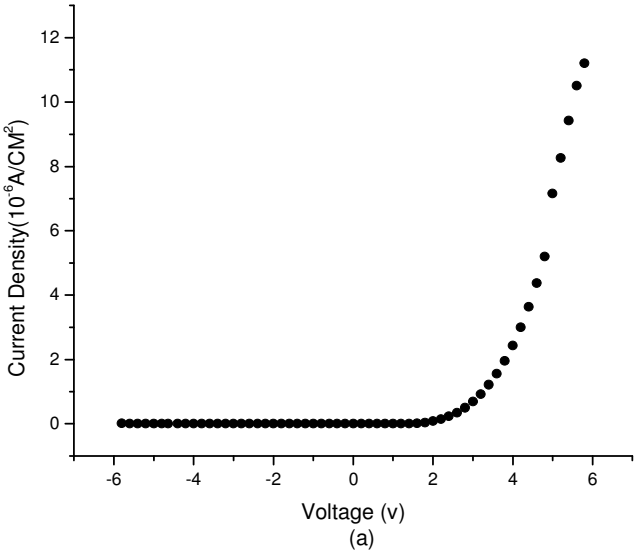

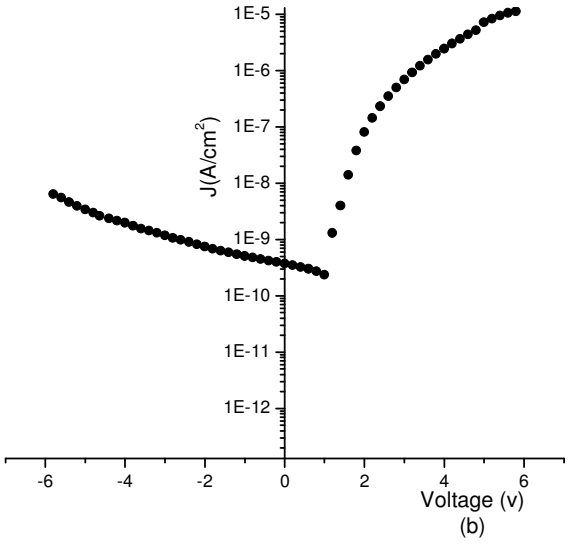

Fig. 6. 2. (a) current density (J)-voltage (V) characteristics, (b) logJ-V of poly[3-(2'-butyloxy-5'-(1'''-oxoocyl)phenyl)thiophene].

A semi-logarismic plot (Fig. 6.2) of the log(J) verses the applied voltage (V) indicates that the current-voltage dependence is an exponential between 0.8V and 2V. This exponential

dependence confirms the formation of a Schottky barrier at the interface between aluminum and the polymer. Under the forward voltage bias greater than 2V the Schottky effect disappears, which is also confirmed by complex spectroscopy measurement (see Section 6.4). Probably the current in this region is due to the bulk resistance of the polymer.

According to the theory of the Schottky barrier (see Section 4.1), the work function of the metal must be smaller than that of p-type semiconductor and a rectifying junction would be formed at the interface. If the work functions were in the reverse order, an ohmic contact would exist rather than a rectifying behavior. We have seen that polymer/Al contact forms a rectifying junction. Thus, the polymer is p-type semiconductor and the work function of Al is less than that of the polymer. The polymer/ITO junction is obviously ohmic. Therefore, the work function of the polymer is in between almunium (4.2 eV) and ITO (4.9 eV).

The rectifying J-V behavior of Schottky barrier device is usually assumed to follow the standard thermionic emission theory for conduction across the junction. And current-voltage relationship for the Schottky barrier device is given by equation 4.2 (see Section 4.2). According to this equation, when $\frac{qV}{KT} >> 1$, we can neglect the term (-1) in the diode equation, and ln(J) verses V is expected to be linear in the vicinity of the turn-on forward voltage. The logJ-V curve (Fig. 6.2(b)) shows this behavior between 0.8V and 2V. Extrapolating the linear plot to zero bias gives the intercept of J corresponding to saturation current density J_o (see Table 5.1).

The barrier height ϕ_b for Schottky diode is related to the saturation current density using

Richardson equation (equation 4.3 in Section 4.2). By assuming the effective Richardson constant (A^*) to be 120A/cm^{2}k^2, which is Richardson constant for a free electron and usually assumed for [9, 44], the Schottky diode with p-type organic semiconductor, and temperature to be at room temperature, the barrier height is calculated to be 1.11eV. Ideality factor (n) can be calculated by obtaining linear slope of logJ against V plot for forward bias and using the relation

$$n = \frac{1}{\left(\frac{KT}{q}\right)\left(\frac{\Delta \ln(J)}{\Delta V}\right)}. \qquad 6.1$$

The ideality factor (n), using equation 6.1, is found to be 3.5. For ideal Schottky diode n = 1. However, n value can be larger than two. This may be due to other charge transport mechanism, such as tunneling, recombination of electrons and holes, and leakage currents.

Table 6. 1 Parameters extracted from Fig. 6.2.

γ	ϕ_b (eV)	n	J_o (A/cm^{-2})
1761	1.11	3.5	2.2x10^{-13}

γ, ϕ_b, n, and J_o are the rectification ratio, barrier height, ideality factor, and saturation current density, respectively.

6.3 Capacitance-Voltage Measurements

Figure 6.3 (a) shows the C-V plot at frequency of 280Hz of Al/the polymer/ITO of the Schottky diode. According to Mott-Schottky theory, it is well known that the depletion layer capacitance per unit area of MS contact can be given by equation 4.4 and simple rearrangement leads to equation 4.5. From equation 4.5, the C^{-2} verses V plot is a straight line. However, the plot is not a straight line in all voltage range (see Fig 6.3 (a)). Deviation from a

straight line may be due to variable impurity concentration. Generally, dopant concentration (N_a) depends on the biasing voltage. However, for small reverses bias voltage (Fig. 6.3 (b)), C^{-2} verses V plot is a straight line, which indicates that dopant density is uniform in the polymer in this voltage range and can be attributed to the formation of depletion region.

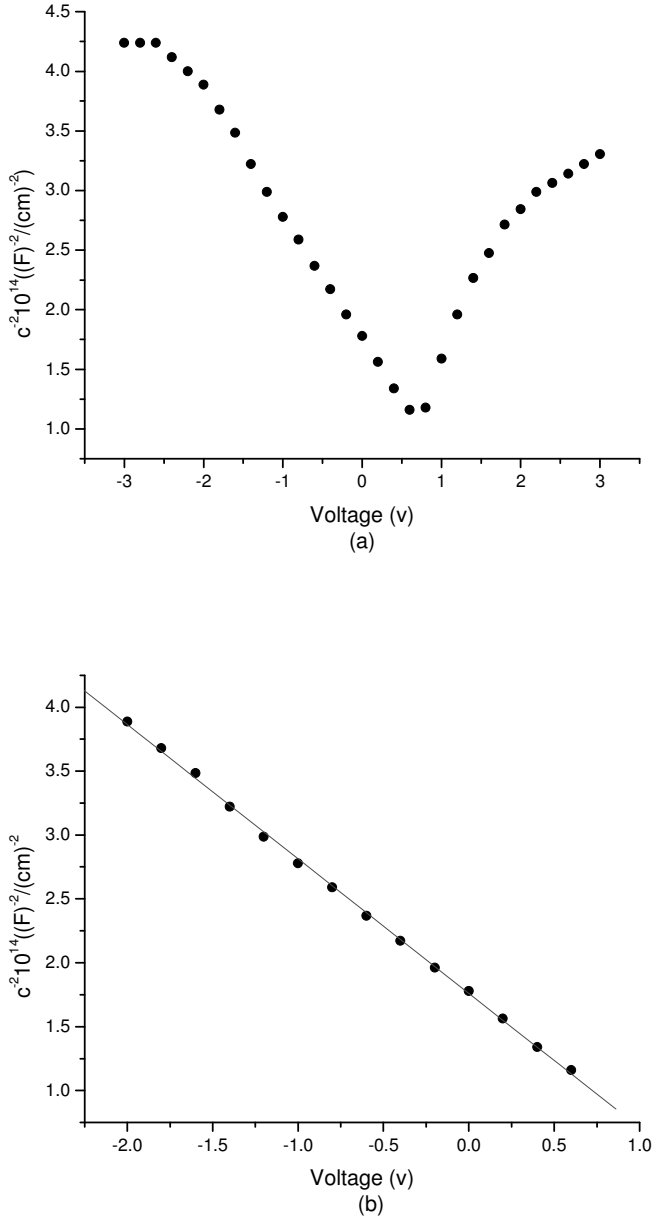

Fig. 6. 3. Capacitance-voltage characteristics of poly[3-(2'-butyloxy-5'-(1'"-

oxoocyl)phenyl)thiophene].

From the plot of C^{-2} verses reverse bias voltage (Fig. 6.3 (b)) the charge carrier concentration (N_a) can be obtain using

$$N_d = -\left(\frac{2}{eA^2{}_s\varepsilon_r\varepsilon_o}\right)\left[\frac{d\left(C^{-2}\right)}{dV}\right]^{-1}, \qquad 6.2$$

where $\frac{d\left(C^{-2}\right)}{dV}$ is the slope of the linear part of the curve (Fig. 6.3 (b)). Inserting the relative permitivity of the polymer ε_r (=3) [40], the permitivity of free space ε_o (=8.8542x10^{-14} F/cm), electronic charge e (=1.6x10^{-19}c), and slope, gives the dopant concentration (see Table 6. 2). Moreover, extrapolating linear part of C^{-2} verses V plot to $1/C^2 = 0$ gives the built-in voltage (V_{bi}) at the abscissa (Table 6.2). Having V_{bi} and dopant concentration, the depletion width at zero bias given by equation 4.6 is also calculated, see Table 6.2.

The separation of Fermi level from the valance band edge (E_V-E_F) in the polymer can be estimated from the relation [37]

$$p_o = N_V \exp\left[\frac{E_V - E_F}{kT}\right], \qquad 6.3$$

by assuming N_V (effective density of states at the top of the valance band) is 10^{21}cm^{-3} [3] and all acceptors being ionized, i.e., $p_0 \approx N_a \approx 4.83\times10^{17}\,cm^{-3}$ (see table 6.2). Since the Fermi level is close to the valance band, the polymer is a p-type semiconducting polymer.

Table 6. 2 Parameters extracted from Fig 6.3

N_a (cm^{-3})	V_{bi} (V)	W (nm)	E_V-E_F(eV)
$4.83x10^{17}$	0.96	25.7	0.18

N_a, V_{bi}, and W are the dopant concentration, built-in voltage, and depletion width, respectively.

6.4 Complex Impedance Analysis

Complex impedance measurement provides some information about the bulk resistance and Schottky barrier junctions [41-43]. So we characterized the sandwich structure device (Fig. 5.2 (b)) by measuring complex impedance as a function of frequency and bias voltage. The Cole-Cole plots of the device at different bias voltages are shown in the Fig. 6.4. The frequency range used in measuring impedance, was between 300 Hz and 100 kHz. At each bias voltage of –6V, -5V, 5V, and 6V, the same frequency range was used. The filled points are the measured coordinates of the real and imaginary parts of the impedance.

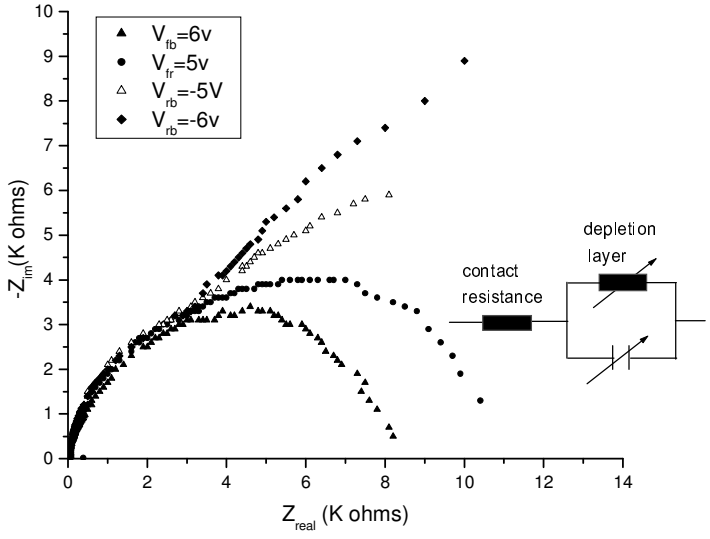

Fig. 6. 4. Cole-Cole plots of Al/polymer/ITO sandwich structure. V_{fb} and V_{rb} are forward and reverse bias voltages, respectively.

The Cole-Cole plots of the complex impedance are semicircles whose center lies on real axis. However, generally the Cole-Cole plots of a device may not be a single semicircle [41, 43], and see Section 4.4. The plot being a semicircle (see Fig. 6.4) at a given voltage may be attributed to absence of resistive insulating layer at the interface. It also helps in modeling the Schottky barrier diode to an equivalent parallel RC circuit shown in the insert of Fig. 6.4. Clearly, the semicircles show bias voltage dependence (Fig. 6.4). The diameters of the semicircles correspond to ohmic resistances. Using this concept the ohmic resistances for each applied bias are determined and listed in Table 6.3. These values decrease with the increase of bias voltage from reverse bias to forward bias and it is consistent with the J-V curve. The contact resistance, which is obtained from the intersection of the semicircles with real axis of the impedance, is bias independent and has the same value for all bias voltages, (Table 6.3).

By circular fitting to our data we extracted parameters. The relation

$-Z_{imag}=(2\pi fC)^{-1}$ is used to estimate the value of capacitance of Schottky barrier at different bias voltages, where f is the frequency at maximum value of $-Z_{imag}$. Substituting these values into $W = \frac{\varepsilon_r \varepsilon_o}{C/A}$, the depletion widths for different bias voltages are calculated, where the relative permitivity $\varepsilon_r = 3$ [40] for polymers is used. All calculated parameters are listed in Table 6.3. Clearly, the depletion widths, the resistances, and capacitances are consistent with J-V curve. At forward bias voltages the thickness of the depletion region indicating the Schottky effect disappeared and at reverse bias voltages thickness is relatively high, and the current transport across the junction is diminished by Schottky barrier.

Table 6. 3 Parameters extracted from Fig. 6.4.

Bias voltage V_b (V)	R_c(Ω)	R_s (kΩ)	Capacitance ($nFcm^{-2}$)	Depletion width (nm)
-6	50	70	47	57
-5	50	60	59	45
5	50	12	325	8
6	50	8	487	5

R_s and R_c are series and depletion region resistances, respectively.

The negative values of V_b are reverse bias voltages.

7.Conclusion

In conclusion, we have studied absorption spectrum of poly[3-(2'-butloxy-5'-(1'''-ocooxyl)phenyl)thiophene] and electrical properties of junctions between the polymer and a low work function metal (Al). The absorption spectrum shows that the polymer is an organic semiconducting polymer with energy gap of 2eV. The J-V curve characteristics of ITO/polymer/Al sandwich structures reveals a rectifying characteristic with the rectification ratio of 1761 at ± 5.6V. Thermionic emission equation has been applied to interpret the current-voltage characteristics of the diode. The contact between the polymer film and aluminum was observed to form a Schottky barrier with potential barrier height of 1.11eV and diode quality factor of 3.5. The saturation current density (J_o= $2.2x10^{-13}$A/cm^2) is small and it indicates good rectification. The polymer is p-type semiconducting polymer since the Fermi level is close to valance band. The C-V data manifest that dopant concentration is inhomogeneous. However, its linear part indicates dopant concentration for small reverse bias voltage (near zero) is uniform and this may be attributed to the formation of depletion region. The Cole-Cole plots of complex impedance spectroscopy of ITO/polymer/Al sandwich structures are single semicircles at different bias voltages, which indicates the absence of an interfacial resistive layer. Moreover, the plot helps to model the Schottky barrier equivalent circuit as parallel RC circuit. The diameter of the semicircles decreases as bias voltage increases from reverse to forward bias, in agreement with its J-V relationship. Finally, the junction may be considered as a metal-semiconductor contact.

In view of a good rectification, this polymer may manifest photovoltaic properties, which should be characterized in the future.

References

[1] H. Shirakawa, E. J. Louis, A. G. MacDiarmid, C. K. Chiang, A. J. Heeger, *Chem.*

Commun. **578** (1977).

[2] C. K. Chiang, Fincher. J_r., Y. W. Park, A. J. Heeger, H. Shirakawa, E. J. Louis, *Phys. Rev*. *Letter.* **39** (1977) 1098.

[3] S. Glenis, G. Ttourillon and F. Garnier, *Thin Solid Films*, **139** (1986) 221.

[4] G. Horocuitz and F. Garnier, *Sol. Energy Mater*, **13** (1986) 47.

[5] H. Koezuka and A. Tsumura, *Synth. Met*. , **28** (1983) C753.

[6] S. A. Chen and H. T. Lee, *Synth. Met*., **47** (1992) 233.

[7] J. C. Chiang and A. G. MacDiarmid, *Synth. Met*., 13 (1986) 193.

[8] J. C. W. Chien, Polacetylene: *Chemistry, Physics, and Material science, Acadamic Press*, Orlando, FL, 1984, p.581.

[9] H. Tomozawa, F. Braun, S. Phillps, A. J. Heeger and H. Kroemer, *Synth, Met*., **22** (1987) 63.

[10] E. H. Rhoderick and R. H. Williams, *Metal-Semiconductor Contacts*, Clarendon Press, Oxford, 1978.

[11] Q. Pei, G. Yu, C. Zhang, Y. Yang, A. J. Heeger, *Science,* **269** (1995) 1086.

[12] M. Berggren, O. Inganas, G. Gustafsson, J. Rasmusson, M. R. Andersson, T. Hjertberg and O. Wennerstrom, *Nature*, **372** (1994) 444.

[13] J. C. Gustafsson, B. Liedberg, and O. Inganas, *Solid State Ionics,* **69** (1994) 145.

[14] C. K. Chiang, C. R. Fincher, J_r., Y. W. Park, A. J. Heeger, H. Shirakawa, E. J. Louis, S. C. Gau, and A. G. MacDiarmid, *Phys. Rev*, Lett., **39**, 1098-1101 (1977).

[15] S. Roth, *One-dimensional Metals*, VCH Publishing Inc., New York, (1995).

[16] N. W. Aschcroft and N. D. Mermin, *Solid State Physics*, Holt, Rinchart and Winston, N.Y., (1976).

[17] Bantikassegn Workalemahu. *Ph. D Dissertation*, ISBN 91-7871-803-1, Linkoping

University, Sweden, 1996, and references cited therein.

[18] W. P. Su, J. R. Schrieffer, and A. J. Heeger, *Phys. Rev*. B **22**, 2099-2111 (1980); (E) B **28**, 1138 (1983).

[19] H. Takayama, Y. R. Lin-Liu, and K. Maki, *Phys. Rev*., B **21**, 2388-2393 (1980).

[20] S. Kivelson, *Phys. Rev.lett*., **46**, 1344-1348 (1981).

[21] A. J. Heeger & J. R. Schrieffer, *Solid State Commun*., **48**, 207-210 (1983).

[22] S. Stafstrom & R. A. Chao, *Phys. Rev*., B **30**, 2098-2103 (1984).

[23] W. P. Su, J.R. Schrieffer, and A. J. Heeger, *Phys. Rev Lett*., **42**, 1698-1701 (1979).

[24] M. Nakahara & K. Maki, *Phys. Rev*., B **25**, 7789-7797 (1982).

[25] K. R. Subbaswamy M. Grabowski, *Phys. Rev*., B **24**, 2168-2173 (1981).

[26] D. K. Campbell, T. A. Degrand, and S. Mazumber, *Phys. Rev. Lett*., **52**, 1717-1720 (1984).

[27] N. Suzuki, M. Ozaki, Etemad, A. J. Heeger, and A. G. Macdiarmid, *Phys. Rev. lett.,* **45**, 1209-1213 (1980); (E) **45,** 1463 (1980).

[28] YuLu, *Solitons and Polarons in Conducting Polymers*, World Scientific Publishing co. Pt. Ltd., (1988).

[29] W. Bantikassegn and O. Inganas, *Synth. Met*., **87** (1997) 5.

[30] J. L. Bredas, J. C. Scott, K. Yakushi, and G. B. Streat, *Phys. Rev*., B **30** (1984) 1023.

[31] R. R. Chane, J. L. Bredas and R. Silbey, *Phys. Rev.,* B **29** (1984) 4491.

[32] E. Punk M. F. Runner, J. L. Hettinger, J. S. Brooks and S. T. Hannahs, *Phys, Rev*., B **43** (1991) 9076.

[33] K. Ehinger and S. Roth, *Phil. Mag*., B **53** (1986) 301.

[34] C. Kittel, *Introduction to Solid State Physics*, 5thed, Wiley Eastern Limited,New York (1976).

[35] C. O. Yoon, M. Reghu, D. Moses and A. J. Heeger, *Phys. Rev*., B **49** (1994) 1085.

[36] P. Sheng, *Phys. Rev*., B **21** (1980).

[37] S. M. Sze, *Physics of Semiconductor Devices*, Wiley, New York, (1981).

[38] W. Bantikassegn, P. Dannetun, O. Inganas, and W. R. Salanech, *Thin solid films*, **224** (1993) 332.

[39] M. Granstrom, M. Berggren, O. Inganas, *Synth. Met*., **76** (1996) 141.

[40] J. R. Macdonald, ed., *Impedance Spectroscopy*, *Emphasizing Solid Materials and Systems*, John Wiley &Sons, New York, (1987).

[41] W. Bantikassegn, O. Inganas, *Thin Solid Films*, **293** (1997) 138.

[42] W. Bantikassegn ,*SINET:Ethiop.J.Sci*.,21(1):51-66,1998.

[43] W. Bantikassegn and O. Inganas, *J. Phys. D: Appl. Phys*. **29** (1996) 2971.

[44] H. Koezuka and S. Etoh, *J. Appl. Phys*., **54** (1983) 2511.